Long non-coding RNA LOC284454 promotes hepatocellular carcinoma cell invasion and migration by inhibiting E-cadherin expression

LILI HAN[1], WEIXIAO ZHOU[2] and FEI WU[1]

[1]Department of Oncology, [2]Clinical Laboratory, The Second Affiliated Hospital, Xi'an Jiaotong University, Xi'an, Shaanxi 710004, P.R. China

Received August 22, 2020; Accepted December 21, 2020

DOI: 10.3892/or.2021.7956

Abstract. Numerous studies have elucidated the impact of long non-coding (lnc)RNAs in carcinogenesis; however, the role and the mechanism of the lncRNA LOC284454 in hepatocellular carcinoma (HCC) remain unknown. In the present study, reverse transcription-quantitative PCR assay, χ^2 analysis and Kaplan-Meier analysis were performed to assess the role of LOC284454 in HCC. Furthermore, MTT and Transwell assays were performed to measure the function of LOC284454 on HCC cell proliferation, invasion and migration. RNA immunoprecipitation, chromatin immunoprecipitation, RNA pull-down, fluorescence *in situ* hybridization and luciferase reporter assays were performed to explore the mechanism of LOC284454. The results revealed that LOC284454 expression was aberrantly elevated in HCC and increased LOC284454 expression was markedly associated with aggressive clinicopathological factors and shorter survival time in patients with HCC, suggesting that LOC284454 behaved as an oncogenic factor in HCC. Mechanistically, LOC284454 could bind with the enhancer of zeste homolog 2 (EZH2) mRNA and subsequently inhibit E-cadherin expression by binding to its promoter region. The rescue assay demonstrated that E-cadherin was essential for the oncogenic function of LOC284454 in HCC cells. The present results suggested that the LOC284454/EZH2/E-cadherin axis may be an alternative therapeutic target for patients with HCC.

Correspondence to: Professor Lili Han, Department of Oncology, The Second Affiliated Hospital, Xi'an Jiaotong University, 157 Xiwu Road, Xi'an, Shaanxi 710004, P.R. China
E-mail: hanlili621@mail.xjtu.edu.cn

Abbreviations: lncRNAs, long non-coding RNAs; HCC, hepatocellular carcinoma; CRC, colorectal cancer; NPC, nasopharyngeal carcinoma; EMT, epithelial-mesenchymal transition; RBP, RNA-binding protein; EZH2, enhancer of zeste homolog 2; OS, overall survival; PRC2, polycomb repressive complex 2

Key words: lncRNA LOC284454, HCC, EZH2, E-cadherin

Introduction

Hepatocellular carcinoma (HCC) is a frequently occurring malignant tumor, with more than half a million new patients being diagnosed each year worldwide (1). Importantly, owing to high metastasis and limited treatment options, patients with HCC usually suffer from a poor prognosis (2). Hepatitis virus infection may be partially responsible for the occurrence of HCC (3); however, the exact underlying molecular mechanism is complex and not entirely clear. Thus, further study of the pathogenesis of HCC is pivotal for providing more therapeutic options and improving the survival of patients with HCC.

Long non-coding RNAs (lncRNAs), which are >200 nucleotides in length, are involved in multiple biological activities and pathological processes by regulating a range of genes at the transcriptional or posttranscriptional level (4,5). Recently, numerous studies have attempted to determine the impact of lncRNAs in carcinogenesis. Liao *et al* (6) reported that the lcnRNA LGMN is significantly upregulated in glioblastoma tissues, and that increased LGMN expression facilitates glioblastoma growth and metastasis. lncMat2B was confirmed to promote cisplatin resistance by facilitating DNA damage repair in breast cancer cells (7). Elevated lncRNA H19 expression was reported to be associated with the metastasis of colorectal cancer (CRC) via upregulation of heterogeneous nuclear ribonucleoprotein A2B1 and Raf-1 expression (8). lncRNA LOC284454 is a stable chromatin-associated lncRNA and seems to be differentially regulated in different types of cancer. For example, LOC284454 expression is markedly downregulated in various types of human cancer, including prostate, breast and kidney cancer (9). However, in nasopharyngeal carcinoma (NPC), oral cancer and thyroid cancer, LOC284454 expression is significantly upregulated (10). A recent study revealed that increased LOC284454 expression indicates a poor prognosis in NPC and facilitates NPC cell migration and invasion (11). However, the role of LOC284454 in HCC has not been investigated.

E-cadherin serves a critical role in regulating cellular adhesion and represses metastasis of human cancers by blocking

epithelial-mesenchymal transition (EMT), which is critically responsible for tumor metastasis (12,13). Our previous study suggested that autophagic degradation of E-cadherin induces EMT and promotes HCC metastasis (14). Consistent with this finding, Zhou *et al* (15) observed that decreased E-cadherin expression in HCC caused by overexpression of plant homeodomain finger protein 8 promotes HCC metastasis.

The RNA-binding protein (RBP) enhancer of zeste homolog 2 (EZH2) acts as a histone inhibitor and significantly contributes to the regulation of its target genes by influencing automethylation (16). Previous studies have revealed that lncRNAs regulate their target genes by binding with RBPs, including EZH2 (17,18). It has been reported that CRNDE lncRNA suppresses its target gene dual-specificity phosphatase 5 by regulating EZH2 expression in CRC (17). Similarly, Linc00460 inhibits cell proliferation and induces apoptosis by repressing its target gene Kruppel-like factor 2 in CRC (18).

The present study aimed to assess the role and mechanism of LOC284454 in HCC cell migration and proliferation. The assays were performed to determine whether LOC284454 may serve as a promising biomarker and novel therapeutic target for patients with HCC.

Materials and methods

HCC and noncancerous tissue specimens. The present study complied with the principles of the Declaration of Helsinki and was approved by the Ethics Committee of Xi'an Jiaotong University (Xi'an, China). A total of 90 paired human cancer and noncancerous tissue specimens (≥2 cm away from the tumor margin) were collected from patients who were histopathologically and clinically diagnosed with HCC and who underwent surgical excision between January 2013 and January 2018 at the Second Affiliated Hospital of Xi'an Jiaotong University. The samples were retained in liquid nitrogen after operation. The clinicopathological characteristics of the patients (median age, 55 years; age range, 30-69 years) are listed in Table I. Tumor stages were determined according to the 2002 American Joint Committee on Cancer/International Union against Cancer Tumor/Lymph Node Metastasis/Distal Metastasis (TNM) classification system (19,20). The longest follow-up duration of the patients was 90.1 months. The overall survival (OS) rate of all patients was 25.6% at 5 years. Receiver operating characteristic curve analysis determined that the cut-off value of LOC284454 was 3.27. The cohort of patients with HCC with LOC284454 expression >3.27 were designated as the LOC284454-high group, and the cohort of patients with LOC284454 expression <3.27 was designated as the LOC284454-low group. A total of 15 human non-tumor liver samples were collected at the Second Affiliated Hospital of Xi'an Jiaotong University in October 2020. None of the individuals had HCC or other malignancies Table SI shows the clinical characteristics of these individuals (median age, 36 years; age range, 27-57 years).

Cell lines and cell culture. The FuHeng Cell Center provided the normal hepatocyte cells (THLE-2 cells), the human liver carcinoma cells (HepG2, Hep3B and MHCC-97L cells) and 293T cells. The cells were grown in DMEM (Invitrogen; Thermo Fisher Scientific, Inc.) with 10% FBS (Gibco; Thermo Fisher Scientific, Inc.) in an incubator at 37˚C with 5% CO_2, and STR profiling was used for authentication.

LOC284454 and EZH2 overexpression lentiviral vectors, and short hairpin (sh)RNA-encoding lentiviral vectors directed against LOC284454, E-cadherin and EZH2 and their respective non-targeting negative control (NC) vectors were designed and provided by Shanghai GenePharma Co., Ltd., with the following sequences: LOC284454 target vector, 5'-GCAGCUUUUCAGAAAUCU-3' and NC vector, 5'-TCG TACTCGTCTTCGAT-3'; E-cadherin target vector, 5'-GGU GGAGGAAGGA CCAUUA-3' and NC vector, 5'-AUAGCC CUGUAAUGCUUU-3'; EZH2 target vector, 5'-GGACCA UUAUAUUCCUUA-3' and NC vector, 5'-AGUGAAACC UUGGCUAGCU-3'. Lentiviral transfection was conducted according to the manufacturer's protocol. When MHCC-97L or Hep3B cells seeded in 6-well plates reached 70% confluence, a total of 0.5 μg lentiviral construct and 10 μg polybrene (Sigma-Aldrich; Merck KgaA) were added to the medium. An MOI value of 10 was used for ov-LOC284454 and ov-EZH2, and an MOI of 8 for the others lentiviral vectors. After 12 h, the medium was replaced with fresh medium containing 1 μg/ml puromycin. Subsequently, the cells were collected after 72 h for further experiments.

Reverse transcription-quantitative PCR (RT-qPCR). TRIzol® reagent (Invitrogen; Thermo Fisher Scientific, Inc.) was used to extract RNA from specimens or cells. The RNA was then reverse transcribed into cDNA using the PrimeScript RT Reagent kit (Takara Bio, Inc.) according to the manufacturer's protocol, and Oligo dT was used as a complementary universal primer. Subsequently, qPCR experiments were performed using the SYBR Premix kit (Takara Bio, Inc.). The relative mRNA expression against GAPDH expression was assessed using $2^{-\Delta\Delta Cq}$ method (21). The optimal results were obtained when the amplification curve exhibited a typical S-type amplification and the curve was smooth. The reaction conditions were as follows: One cycle of preheating for 10 min at 92˚C, followed by 40 cycles at 90˚C for 15 sec, 55˚C for 50 sec and 70˚C for 30 sec, and finally one cycle at 97˚C for 90 sec, 60˚C for 3 min and 94˚C for 10 sec. The primer sequences are shown in Table SII.

MTT assays. Parental and transfected MHCC-97L or Hep3B cells were seeded into 96-well plates (2,000 cells/well). A total of 15 μl MTT was added to each well at the indicated time points (0, 24, 48 or 72 h). The cells treated with MTT were then incubated for another 4 h at room temperature, and the solution in each well was replaced with fresh medium containing 150 μl DMSO. The results were measured at an absorbance of 492 nm using a microplate reader (BioTek Instruments, Inc.; Agilent Technologies, Inc.).

Western blotting. The concentration of the protein samples extracted from MHCC-97L or Hep3B cells using RIPA lysis buffer (Thermo Fisher Scientific, Inc.) was measured using a BCA kit (Beyotime Institute of Biotechnology). The protein samples (25 μg/lane) were resolved via 4-20% SDS-PAGE (GenScript), electronically transferred to PVDF membranes, blocked in 5% skimmed milk at 37˚C for 1 h and

Table I. Association between LOC284454 expression and clinicopathological features in patients with hepatocellular carcinoma.

Variable	Total number of patients, n (%)	LOC284454, n		P-value
		Low expression	High expression	
Age, years				0.479
<50	37 (41.1)	15	22	
≥50	53 (58.9)	20	33	
Sex				
Female	13 (14.4)	4	9	0.373
Male	77 (85.6)	31	46	
Tumor size, cm				0.033[a]
<5	35 (38.9)	9	26	
≥5	55 (61.1)	26	29	
Tumor multiplicity				0.040[a]
Single	64 (71.1)	29	35	
Multiple	26 (28.9)	6	20	
Microscopic vascular invasion				<0.01[b]
No	51 (56.7)	33	18	
Yes	39 (43.3)	2	37	
Stage				<0.01[b]
I-II	51 (56.7)	33	18	
III-IV	39 (43.3)	2	37	

[a]P<0.05; [b]P<0.01.

incubated overnight at 4˚C with the appropriate primary antibodies, including anti-E-cadherin (1:500; cat. no. 14472), anti-N-cadherin (1:300; cat. no. 13116), anti-vimentin (1:300; cat. no. 574), anti-EZH2 (1:500; cat. no. 5246) and anti-GAPDH (1:3,000; cat. no. 5174). The primary antibodies were all purchased from Cell Signaling Technology, Inc. Protein expression levels were normalized to those of the internal control (GAPDH). Subsequently, the membranes were incubated with goat anti-rabbit secondary antibodies (cat. no. bs-40295G-IRDye8) for E-cadherin, N-cadherin, vimentin and EZH2, and goat anti-mouse secondary antibodies (cat. no. bs-40296G-IRDye8) for GAPDH (both 1:10,000; BIOSS) at 37˚C for 2 h. The intensity of the protein signal was observed using an ECL Detection System (Thermo Fisher Scientific, Inc.). ImageJ version 1.6.0 software (National Institutes of Health) was used to quantify the intensity of the protein bands.

Transwell assays. Transwell chambers (8-μm; EMD Millipore) were used for examining cell migration and invasion. To measure cell invasion, the membranes were precoated with 200 mg/ml Matrigel® (BD Biosciences) for ~30 min at room temperature. MHCC-97L or Hep3B cells ($1x10^4$) suspended in 200 μl DMEM without FBS were seeded into the upper chambers of Transwell inserts placed in 24-well plates. As the attractant for cell invasion and migration, 600 μl DMEM with 10% FBS was added to the bottom chambers. After incubation for 48 h at 37˚C, the cells that invaded the membrane were stained with 0.1% crystal violet solution (Amresco, LLC) for 30 min at room temperature. The invaded cells in at least three random fields of view at x200 magnification were counted using a fluorescence microscope (Olympus Corporation).

RNA immunoprecipitation (RIP) assays. The EZMagna RIP kit (EMD Millipore) was used to conduct RIP assays according to the manufacturer's instructions. A total of $3x10^7$ MHCC-97L or Hep3B cells transfected with ov-LOC284454 or ov-EZH2 for 48 h were collected and incubated overnight at 4˚C with RIP buffer in the EZMagna RIP kit containing antibody against Argonaute2 (Anti-Ago2; 1:1,000; cat. no. ab32381; Abcam) or anti-IgG (1:1,000; cat. no. ab109489; Abcam) and 5 µg of magnetic beads coated with anti-Argonaute2 (Ago2). After incubation with protease K buffer at 55˚C for 30 min, the immunoprecipitated RNA was extracted using the RNeasy MinElute Cleanup kit (EMD Millipore) and reverse transcribed using Prime-Script RT Master Mix (Takara Bio, Inc.). Finally, the purified RNAs were measured by qPCR assays, as aforementioned. lncDUXAP10 was used as the negative control since it has been shown not to bind with EHZ2 (22).

Chromatin immunoprecipitation (ChIP). ChIP assays were performed using a Pierce Agarose ChIP kit (cat. no. 26156; Pierce; Thermo Fisher Scientific, Inc.) according to the manufacturer's protocol. MHCC-97L or Hep3B cells were collected in a tube for centrifugation at 1,000 x g for 2 min at 4˚C, were then treated with 1% formaldehyde and collected with lysis buffer (cat. no. P0013G; Beyotime Institute of Biotechnology). Ultrasonication (20 KHz; 10 times at room temperature; 10 sec each time with 3 sec intervals) was used to break DNA fragments. The remaining lysates were immunoprecipitated

with normal rabbit IgG antibody (1:500; cat. no. sc-2025; Santa Cruz Biotechnology, Inc.) and then immunoprecipitated with Protein G Agarose Beads and incubated overnight at 4˚C with gentle shaking. Subsequently, DNA crosslinking was performed with buffer made up of 50 mmol/l NaCl, 10 mmol/l KCl and 4.2 mmol/l Na_2HPO_4, and 20 mg/ml Proteinase K, and the DNA was purified with a PCR Purification kit (cat. no. 28104; Qiagen GmbH). Finally, RT-qPCR assays were performed as aforementioned to amplify the precipitated DNAs.

RNA pull-down assay. After the lysates were collected from MHCC-97L and Hep3B cells transfected with a biotin-labeled EZH2-WT or EZH2-MUT probe, which were designed and provided by Shanghai GenePharma Co., Ltd, a pull-down assay was performed using the Pierce Magnetic RNA-Protein Pull-Down kit (Thermo Fisher Scientific, Inc.) according to the manufacturer's protocol. Briefly, 200 μl cell lysates were combined with streptavidin-coated A/G plus magnetic beads (Invitrogen; Thermo Fisher Scientific, Inc.) for 2 h at room temperature. Subsequently, the mixture was centrifuged at 1,000 x g for 1 min at 4˚C and washed with ice-cold washing buffer (20 mM Tris-base pH 7.4, 350 mM KCl and 0.02% NP-40), low-salt buffer and then high-salt buffer. After the beads bound with the magnetic frame, total RNA was extracted using TRIzol and measured via RT-qPCR, as aforementioned.

Fluorescence in situ hybridization (FISH) assay. The Ribo™ FISH kit (Guangzhou RiboBio Co., Ltd.) was used for the RNA FISH assay according to the manufacturer's protocol. MHCC-97L and Hep3B cells were fixed with 4% paraformaldehyde for 10 min at 25˚C, and then permeabilized with 0.5% PBS for 10 min at 4˚C. Next, the cells were blocked with prehybridization buffer for 30 min at 37˚C and then the cells were washed with saline sodium citrate buffer solution and the nuclei were stained with DAPI at 37˚C for 1 min (Beyotime Institute of Biotechnology). The air-dried cells were incubated further with 40 nM of the FISH probe designed and synthesized by Guangzhou RiboBio Co., Ltd., in hybridization buffer at 95˚C for 1 min. Fluorescence was observed using an LSM 880 confocal laser scanning microscope (Zeiss GmbH; magnification, x400). The relative fluorescence intensity was quantified using ImageJ software version 1.51 (National Institutes of Health).

Luciferase reporter assay. 293T cells ($5x10^3$/well) were seeded in a 24-well plate and then co-transfected with *Renilla* luciferase vector (phRL-TK; Promega Corporation), wild-type (wt) LOC284454 or mutant (mut) LOC284454 vector, wt or mut EZH2 vector, and pGL3-E-cadherin-3'-untranlated region reporter vector (Shanghai GenePharma Co., Ltd.). After transfection using Lipofectamine® 2000 (Invitrogen; Thermp Fisher Scientific, Inc.) for 24 h, luciferase activity was measured using the Dual-Luciferase Reporter Assay System (Promega Corporation). The relative luciferase activity was normalized to *Renilla* luciferase activity.

Statistical analysis. SPSS 18.0 software (SPSS, Inc.) was used to perform statistical analyses. The assays were performed three times, and the results are shown as the mean ± SD. χ^2 analyses were performed to analyze the association between clinicopathological features and LOC284454 expression. Kaplan-Meier survival analysis with the log-rank test was conducted to estimate the association between LOC284454 expression and the prognosis of patients. One-way ANOVA with Dunnett's multiple comparisons test was used for comparisons among multiple groups and Student's t-test was used to compare the values between two groups. The comparisons between paired tumor and normal tissues were analyzed with a paired t-test, while comparisons between cells with an unpaired t-test. Spearman's correlation analysis was used to assess the correlation between LOC284454 and E-cadherin expression in HCC. $^*P<0.05$ was considered to indicate a statistically significant difference.

Results

LOC284454 expression is aberrantly elevated in HCC and has prognostic significance in patients with HCC. First, LOC284454 expression was investigated in 90 paired HCC and non-cancerous tissues using RT-qPCR, revealing that LOC284454 expression was significantly elevated in HCC samples compared with in non-cancerous samples ($P<0.05$; Fig. 1A). Furthermore, RT-qPCR analysis suggested that LOC284454 expression was higher in liver cancer cells, including HepG2, MHCC-97L and Hep3B cells, compared with that in normal hepatocytes (THLE-2 cells) ($P<0.05$; Fig. 1B).

To evaluate whether LOC284454 expression had clinical importance in HCC, the association between LOC284454 expression and clinicopathological features of patients with HCC was analyzed. As shown in Table I, the results demonstrated that LOC284454 expression was associated with microscopic vascular invasion ($P<0.01$), tumor multiplicity ($P=0.04$), advanced TNM stage ($P<0.01$) and larger tumor size ($P=0.033$) in patients with HCC. Kaplan-Meier analysis revealed that compared with lower LOC284454 expression, increased LOC284454 expression indicated a shorter OS ($P<0.001$; Fig. 1C) and shorter disease-free survival ($P<0.001$; Fig. 1D) of patients with HCC. A total of 15 human non-tumor liver samples were also collected and RT-qPCR was performed. The results suggested that the expression levels of LOC284454 in human non-tumor liver samples and non-cancerous tissues from patients with HCC were not significantly different (Fig. S1).

LOC284454 promotes HCC cell invasion and migration. LOC284454 expression in MHCC-97L and Hep3B cells was significantly higher than that in THLE-2 cells. The shRNA-encoding lentivirus targeting LOC284454 (sh-LOC284454) or its NC lentivirus (sh-Ctrl) were transfected into MHCC-97L cells and Hep3B cells. RT-qPCR revealed that LOC284454 expression was significantly decreased in cells transfected with sh-LOC284454 compared with those transfected with sh-Ctrl ($P<0.01$; Fig. 2A). Additionally, FISH assays were performed in HCC cells, revealing that LOC284454 was mainly located in the nucleus and that LOC284454 expression was decreased in MHCC-97L cells and Hep3B cells transfected with sh-LOC284454 (Fig. S2). The MTT assay

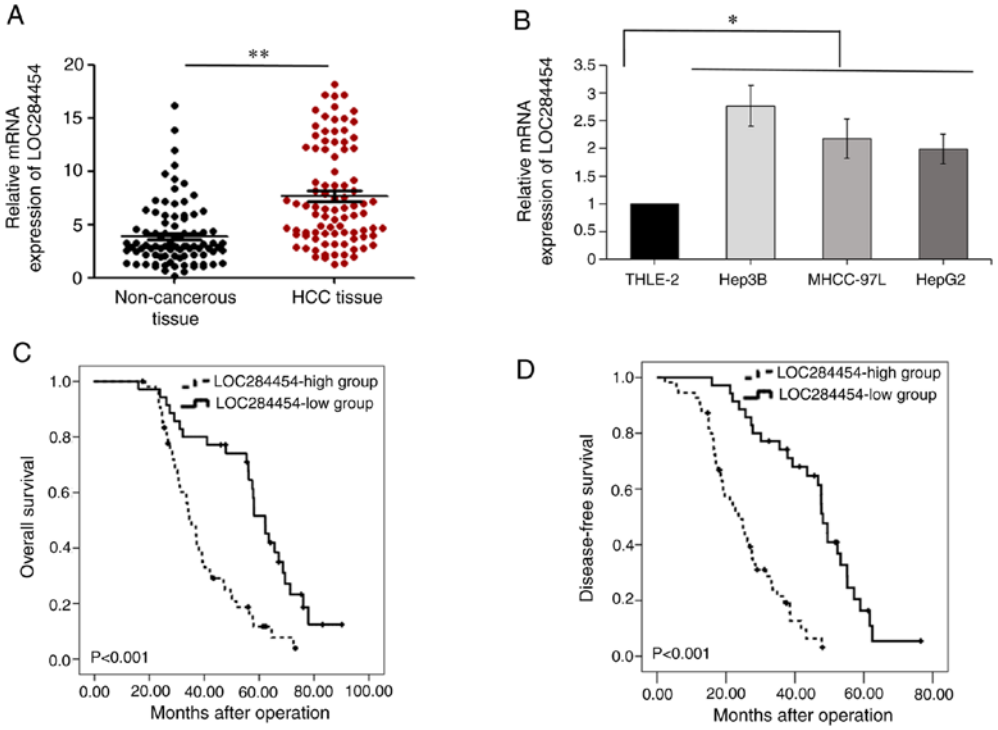

Figure 1. LOC284454 expression is increased in HCC. (A) LOC284454 expression in 90 paired HCC and non-cancerous tissues was analyzed by RT-qPCR. (B) LOC284454 expression in THLE-2 and liver cancer cell lines was tested by RT-qPCR. Kaplan-Meier analysis of (C) the overall survival and (D) disease-free survival of patients with HCC with high and low LOC284454 expression. *P<0.05; **P<0.01. RT-qPCR, reverse transcription-quantitative PCR; HCC, hepatocellular carcinoma.

suggested that MHCC-97L and Hep3B cell proliferation in the sh-LOC284454 group was significantly decreased than that in the sh-Ctrl group (P<0.01; Fig. 2B). In addition, the change in HCC cell migration and invasion induced by the knockdown of LOC284454 was evaluated using Transwell assays. The results confirmed that MHCC-97L and Hep3B cell migration and invasion were significantly decreased by knockdown of LOC284454 (P<0.01; Fig. 2C). These results suggested that LOC284454 enhanced the malignant biological behavior of HCC cells, especially invasion and migration.

EMT is well known as an essential mechanism and primary process of tumor metastasis (23,24). Thus, it was hypothesized that LOC284454 promoted HCC cell migration by inducing EMT. RT-qPCR (Fig. 2D) and western blot analysis (Fig. 2E) were performed to assess the change in the expression levels of EMT markers in MHCC-97L and Hep3B cells. The results indicated that E-cadherin expression was significantly increased by LOC284454-knockdown, while N-cadherin and vimentin expression was not affected (P<0.05; Fig. 2D and E). The current data demonstrated that LOC284454 facilitates migration and invasion by promoting EMT in HCC cells.

LOC284454 inhibits E-cadherin. To identify the mechanism of LOC284454 in HCC, the present study attempted to identify the downstream effector of LOC284454. Downregulation of E-cadherin is essential for EMT, and the current results suggested that E-cadherin expression was significantly affected upon LOC284454-knockdown. RT-qPCR was performed to evaluate the correlation between LOC284454 expression and N-cadherin, vimentin or E-cadherin expression in HCC tissues. Spearman's correlation analysis (Fig. 3A) revealed a significant negative correlation between LOC284454 and E-cadherin expression (P<0.001; r=-0.846); however, there was a positive correlation between LOC284454 and N-cadherin (P=0.001; r=0.352) or vimentin (P<0.001; r=0.373) expression. These results suggested that LOC284454 may enhance EMT of HCC cells by suppressing E-cadherin expression.

LOC284454 binds to EZH2. Numerous studies have elucidated that lncRNAs modulate their target genes by binding with RBPs and polycomb repressive complex2 (PRC2) (25-27). RBP EZH2 is the core subunit of PRC2, is involved in the regulation of lncRNAs on their downstream effectors and participates in the downregulation of E-cadherin in cancer metastasis (28,29). Thus, RIP experiments were performed to assess the interaction between LOC284454 and EZH2. First, the LOC284454 overexpression lentiviral vector (ov-LOC284454) or its NC lentiviral vector (ov-Ctrl) were transfected into HCC cells. RT-qPCR revealed that LOC284454 expression was significantly increased in HCC cells transfected with ov-LOC284454 compared with in those transfected with ov-Ctrl (P<0.01; Fig. 3B). The RIP assay results corroborated the aforementioned hypothesis that LOC284454 could bind to EZH2 in HCC cells (P<0.01; Fig. 3C). Considering that Ago2 is known as a core component of the RNA-induced silencing complex (30), further RIP assays were performed using Ago2 antibodies. Ago2 protein-RNA complexes were precipitated from MHCC-97L and Hep3B cells, and the results revealed that endogenous LOC284454 was preferentially enriched in Ago2 RIPs compared with control IgG antibody RIPs (P<0.01; Fig. S3A). Moreover, Ago2 RIP samples were significantly enriched

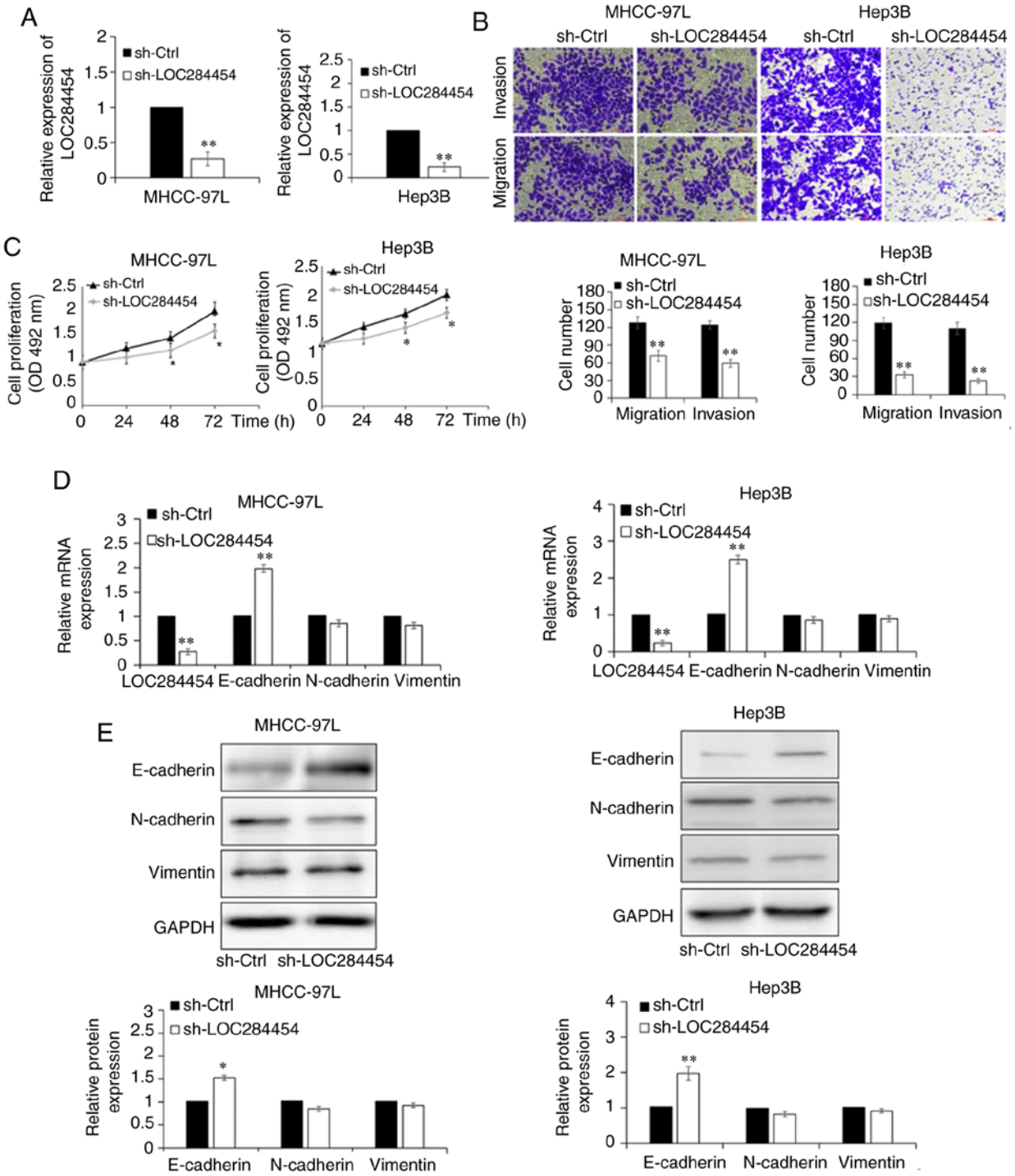

Figure 2. LOC284454 promotes liver cancer cell invasion and migration. (A) RT-qPCR verified that LOC284454 expression was significantly downregulated in MHCC-97L and Hep3B cells transfected with sh-LOC284454. (B) Transwell assay revealed that LOC284454-knockdown inhibited MHCC-97L and Hep3B cell migration and invasion (magnification, x200). (C) MTT assay revealed that LOC284454-knockdown suppressed MHCC-97L and Hep3B cell proliferation. (D) RT-qPCR of the mRNA expression levels of EMT markers in MHCC-97L and Hep3B cells transfected with sh-LOC284454. (E) Western blot analysis of the protein expression levels of EMT markers in MHCC-97L and Hep3B cells transfected with sh-LOC284454. *P<0.05; **P<0.01 vs. sh-Ctrl. RT-qPCR, reverse transcription-quantitative PCR; EMT, epithelial-mesenchymal transition; sh, short hairpin; Ctrl, control; OD, optical density.

for endogenous EZH2, suggesting that LOC284454 and EZH2 may be in the same Ago2 complex in MHCC-97L and Hep3B cells (P<0.01; Fig. S3A). Furthermore, the overexpression EZH2 lentiviral vector (ov-EZH2) or its NC lentiviral vector (ov-NC) were transfected into MHCC-97L and Hep3B cells. RT-qPCR revealed that EZH2 expression was significantly increased in HCC cells expressing ov-EZH2 compared with in those transfected with ov-NC (P<0.01; Fig. 3D). EZH2- mutational lentiviral vectors (EZH2-MUT) were also developed, and RIP assays were performed in which lncDUXAP10 was used as the negative control since it has been shown not to bind with EHZ2 (22). The RIP assays suggested that LOC284454 was more enriched in MHCC-97L and Hep3B cells transfected with the ov-EZH2

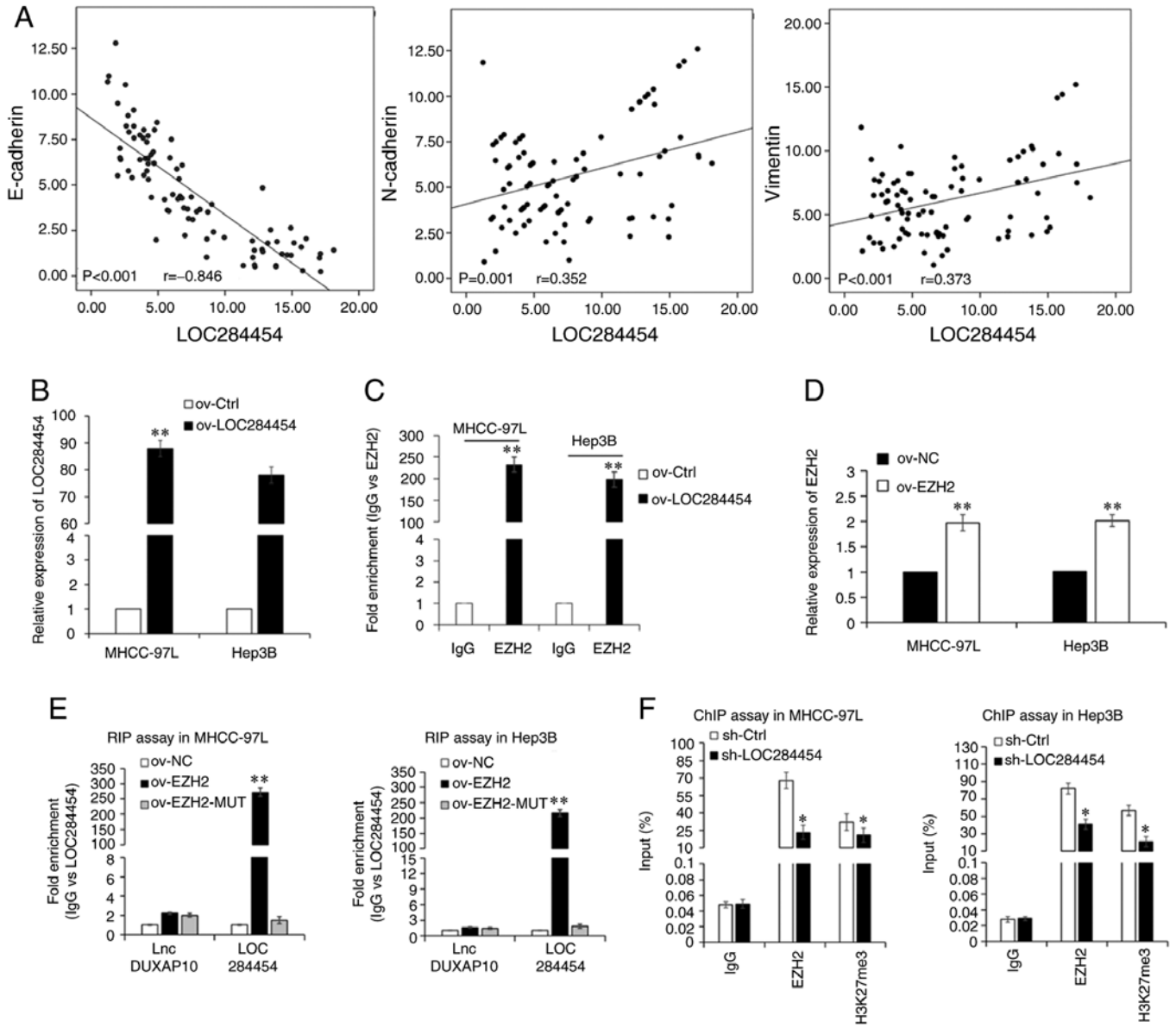

Figure 3. LOC284454 binds with EZH2. (A) Spearman's correlation analysis of the association between the expression levels of LOC284454 and E-cadherin, N-cadherin or vimentin in HCC tissues. (B) RT-qPCR assays were used to analyze LOC284454 expression. (C) RIP assay revealed the enrichment of EZH2 mRNA. (D) RT-qPCR of EZH2 expression in MHCC-97L and Hep3B cells transfected with ov-EZH2. (E) RIP assay revealed the enrichment of LOC284454. (F) ChIP assay revealed whether EZH2 could bind to the E-cadherin promoter. *P<0.05; **P<0.01 vs. Ctrl/NC. RIP, RNA immunoprecipitation; lnc, long non-coding; ov, overexpression; Ctrl, control; NC, negative control; EZH2, enhancer of zeste homolog 2; ChIP, chromatin immunoprecipitation; RT-qPCR, reverse transcription-quantitative PCR; sh, short hairpin.

vector than in those transfected with the EZH2-MUT or ov-NC vector, further suggesting a direct interaction between EZH2 and LOC284454 in HCC cells (P<0.01; Fig. 3E). In addition, biotin-labeled pull-down followed by RT-qPCR analysis revealed that a wt biotin-labeled EZH2 probe (Bio-EZH2-probe-WT) pulled down LOC284454 from the RNA-protein complex, while Bio-EZH2-probe-MUT did not pull down LOC284454 (P<0.01; Fig. S3B). Consistently, the results of the dual-luciferase reporter assays revealed that LOC284454 and EZH2 interacted with E-cadherin (P<0.01; Fig. S3C). To reveal whether LOC284454 could modulate the enrichment of EZH2 in the E-cadherin mRNA promoter region, ChIP assays were performed. The ChIP assay results suggested that LOC284454-knockdown significantly decreased the enrichment of EZH2 in the promoter region of E-cadherin, suggesting that LOC284454 and EZH2 may be enriched in the E-cadherin promoter region (P<0.01; Fig. 3F).

The shRNA-encoding lentiviral vector targeting EZH2 (sh-EZH2) or its NC lentiviral vector (sh-NC) were transfected into MHCC-97L and Hep3B cells. The RT-qPCR results indicated that EZH2 expression was significantly decreased in HCC cells transfected with sh-EZH2 compared with in those transfected with sh-0NC (P<0.01; Fig. 4A). RT-qPCR (P<0.01; Fig. 4A) and western blot analysis (P<0.05; Fig. 4B) suggested that E-cadherin expression was significantly upregulated upon EZH2-knockdown. To investigate whether EZH2 was essential for LOC284454-dependent E-cadherin expression downregulation, the sh-EZH2 lentiviral vector was transfected into MHCC-97L and Hep3B cells overexpressing LOC284454 (ov-LOC284454+sh-EZH2). The results of

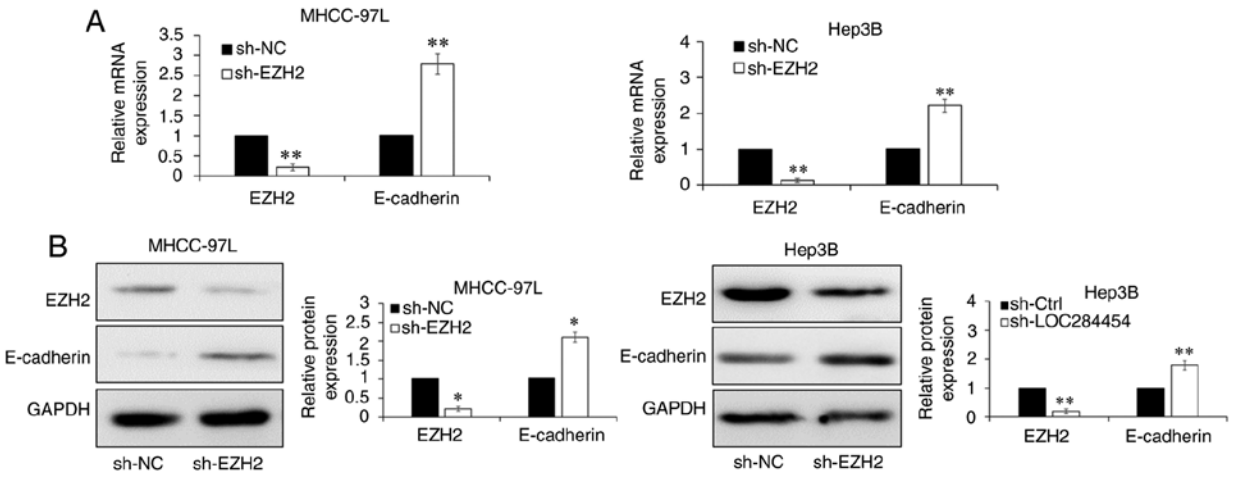

Figure 4. LOC284454 inhibits E-cadherin in liver cancer cells. (A) Reverse transcription-quantitative PCR assays and (B) western blot analysis of EZH2 expression in MHCC-97L and Hep3B cells transfected with sh-EZH2. *P<0.05; **P<0.01 vs. Ctrl/NC. Ctrl, control; NC, negative control; EZH2, enhancer of zeste homolog 2; sh, short hairpin.

RT-qPCR and western blot analysis revealed that LOC284454 and EZH2 expression was increased upon the transfection of ov-LOC284454, and decreased after co-transfection with sh-EZH2 vectors into HCC cells, while E-cadherin expression was not downregulated by overexpression of LOC284454 when EZH2 was knocked down in MHCC-97L and Hep3B cells (Fig. S4). These results demonstrated that LOC284454 suppressed E-cadherin expression by binding with EZH2.

E-cadherin is essential for the oncogenic function of LOC284454. To highlight the significance of E-cadherin in the function of LOC284454, rescue assays were performed. RT-qPCR results confirmed that transfection with sh-E-cadherin significantly decreased E-cadherin expression compared with the negative control group (sh-Ctrl) in MHCC-97L cells and Hep3B cells (P<0.01; Fig. S5). RT-qPCR (P<0.01; Fig. 5A) and western blot analysis (P<0.05; Fig. 5B) revealed that compared with cells transfected with sh-LOC284454+sh-NC, E-cadherin expression was significantly downregulated in LOC284454-knockdown MHCC-97L cells transfected with sh-E-cadherin (sh-LOC284454 + sh-E-cadherin). The MTT assay revealed that cell proliferation was attenuated after E-cadherin expression was downregulated by transfection with sh-E-cadherin in LOC284454-knockdown MHCC-97L cells (P<0.01; Fig. 5C). The Transwell assay revealed that E-cadherin-knockdown reversed the inhibitory effect of LOC284454-knockdown on the invasion and migration of MHCC-97L cells (P<0.01; Fig. 5D). In addition, inhibition of E-cadherin in LOC284454-knockdown Hep3B cells exhibited similar results (Fig. 5E-H). These results strongly suggested that E-cadherin may be essential for the oncogenic functions of LOC284454 in HCC.

Discussion

The present study revealed that LOC284454 expression was aberrantly elevated in HCC tissues and cells, and increased LOC284454 expression was associated with a poor prognosis in patients with HCC. Furthermore, the present results revealed that LOC284454 acted as an oncogenic factor, promoting HCC cell invasion and migration by decreasing E-cadherin expression, which is essential for EMT and metastasis of HCC cells. Mechanistically, LOC284454 could bind to EZH2 mRNA and subsequently inhibit E-cadherin by enriching in its promoter region. Furthermore, rescue assays demonstrated that E-cadherin was essential for the oncogenic functions of LOC284454 in HCC cell invasion and migration. The current results suggested that the LOC284454/EZH2/E-cadherin axis may be a promising therapeutic target for patients with HCC. Previous studies reported that lncRNAs had a significant impact in various types of human cancer, including renal cell carcinoma, HCC and nasopharyngeal carcinoma (4-6). Therefore, the discovery of new hepatocarcinogenesis-associated lncRNAs and further understanding of the role of lncRNAs during the occurrence and development of HCC may help to reveal the pathogenic mechanisms of HCC. Recently, the importance of LOC284454 in human tumors has gained more attention. However, the expression pattern and the importance of LOC284454 in HCC has not been previously reported. The present experiments in HCC samples and cells revealed that LOC284454 expression was aberrantly increased in HCC compared with in normal samples and cells. Further clinical investigation demonstrated that elevated LOC284454 expression predicted more aggressive clinical features and a poor prognosis in patients with HCC. This was in accordance with previous studies that confirmed that numerous lncRNAs are abnormally expressed and are used as independent molecular markers in HCC. For example, the lncRNA SNHG1 was reported to be differentially expressed in HCC and served as an independent molecular marker of HCC [hazard ratio (HR) =2.977] (31). Elevated expression levels of HOXD-AS1 lncRNA was also found in HCC and was found to be associated with a poor prognosis; multivariate regression analysis revealed that HOXD-AS1 expression was an independent and significant factor for OS (HR=1.552) (32). Upregulated lncCSMD1-1 expression was reported to be associated with an advanced stage of HCC and with worse outcomes in patients with HCC (HR=3.80) (33). In the present study, LOC284454 was knocked down in MHCC-97L and Hep3B cells and then MTT and Transwell assays were performed to test the function of LOC284454 in HCC cells. LOC284454 was discovered to

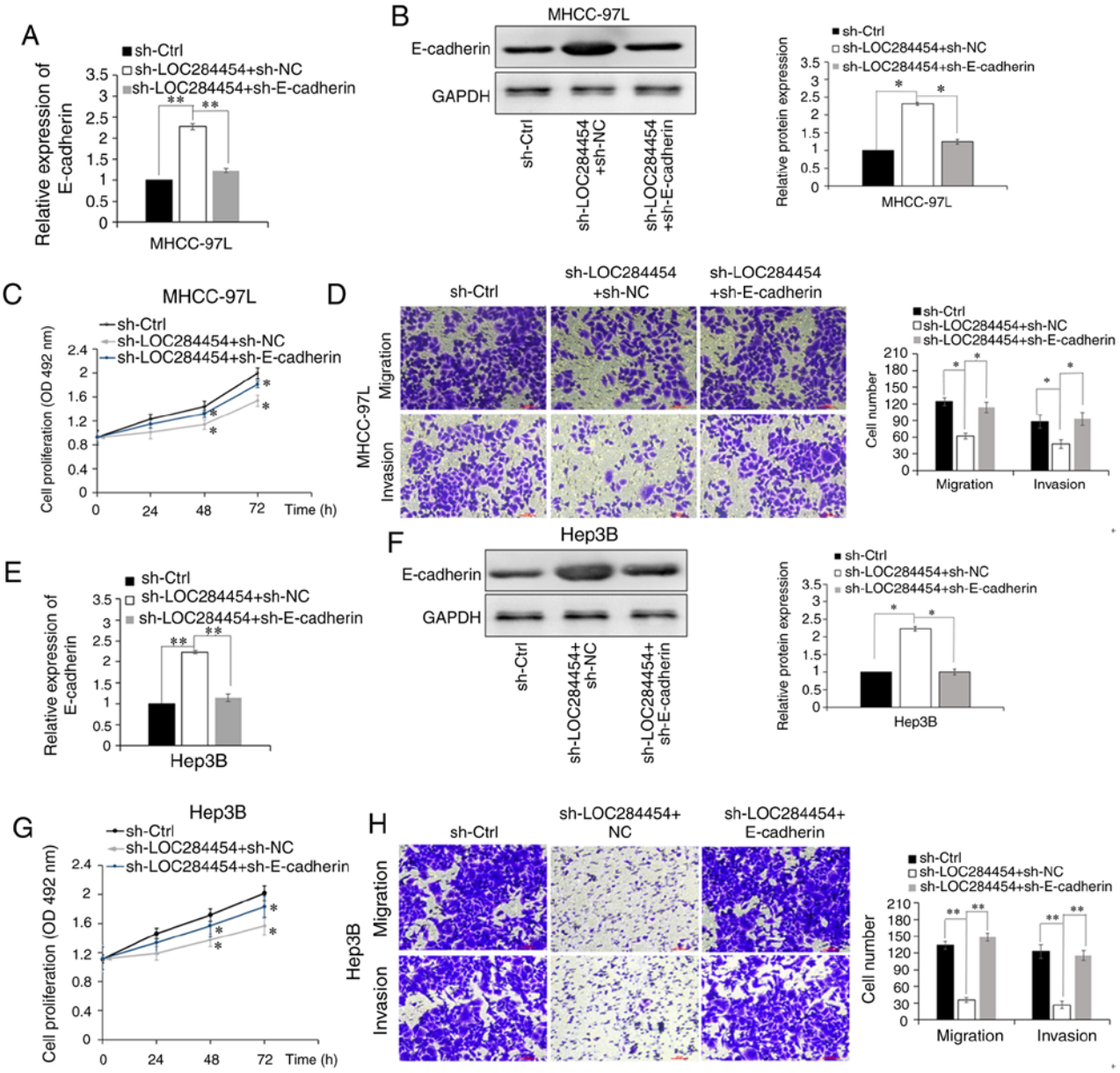

Figure 5. E-cadherin downregulation is essential for the oncogenic function of LOC284454. E-cadherin expression was measured by (A) RT-qPCR and (B) western blotting. (C) MTT assay revealed that inhibition of E-cadherin rescued the effect of LOC284454-knockdown on MHCC-97L cell proliferation. (D) Inhibition of E-cadherin rescued the effect of LOC284454-knockdown on MHCC-97L cell migration and invasion (magnification, x200). E-cadherin expression was measured by (E) RT-qPCR and (F) western blotting in LOC284454-knockdown Hep3B cells transfected with sh-E-cadherin. (G) MTT assay revealed that inhibition of E-cadherin rescued the effect of LOC284454-knockdown on Hep3B cell proliferation. (H) Inhibition of E-cadherin rescued the effect of LOC284454-knockdown on Hep3B cell migration and invasion (magnification, x200). *P<0.05; **P<0.01 vs. Ctrl/NC. Ctrl, control; NC, negative control; sh, short hairpin; RT-qPCR, reverse transcription-quantitative PCR; OD, optical density.

facilitate HCC cell migration, invasion and proliferation. To the best of our knowledge, the present study is the first to reveal that LOC284454 may be of immense importance as a prognostic biomarker in HCC.

There is an increasing amount of evidence that lncRNAs work as pro-tumorigenic or tumor-suppressing factors upon the modulation of their target genes by forming complexes with RBPs (34-36). The present study demonstrated that LOC284454 promoted hepatocarcinogenesis by repressing E-cadherin expression, verifying the association between the pro-tumorigenic effects of LOC284454 and its regulatory effect on E-cadherin. Similar findings in other studies have revealed that numerous lncRNAs serve as oncogenic factors in multiple types of human cancer, such as bladder, gastric and non-small cell lung cancer, by impairing E-cadherin expression at the transcriptional level, including H19 lncRNA, RP11-789C1.1 lncRNA and FEZF1-AS1 lncRNA (37-39). In the present study, RIP assays were performed and confirmed that LOC284454 could bind with EZH2. The RT-qPCR results suggested that LOC284454 and EZH2 inhibited E-cadherin expression. Subsequently, ChIP assays confirmed that LOC284454 could bind with EZH2 and then suppress E-cadherin expression at the transcriptional level. Several other independent studies have also unveiled a direct association and regulation between EZH2 and E-cadherin. Liu *et al* (40) revealed that EZH2 facilitated metastasis and decreased E-cadherin expression in renal cell carcinoma. Additionally, EZH2 was

confirmed to form a complex with histone deacetylase 1/2 and Snail, and then to bind with the E-cadherin promoter with Snail in NPC (41). Linc-UBC1 was reported to promote the metastasis of esophageal squamous cell carcinoma by enhancing EZH2 and then suppressing E-cadherin expression (42). To the best of our knowledge, the current data revealed for the first time that LOC284454 promoted HCC cell migration and invasion by binding with EZH2 and then repressing the downstream target gene E-cadherin.

E-cadherin serves an important tumor-suppressing role in HCC by regulating cell differentiation, polarity, invasion, migration and stem cell-like properties (43,44). The silencing or inhibition of E-cadherin frequently occurs in the initial phases of cancer cell invasion and migration, and has a significant impact on HCC development and metastasis (45). Furthermore, down-regulation of E-cadherin expression in human cancer has been identified as a critical fundamental mechanism and major characteristic of EMT (46). Qiu *et al* (47) reported that E-cadherin expression is decreased or silenced in breast cancer samples and cells, and that P2Y2 receptor-facilitated breast cancer metastasis depends on regulation of E-cadherin. Furthermore, E-cadherin is essential for the microenvironment in tumors by regulating tumor radioresistance and EMT (48). Additionally, E-cadherin was confirmed to participate in the oncogenic function of N-myc downstream-regulated gene-1 and transforming growth factor-β in pancreatic cancer (49). In the present study, a rescue assay was performed and found that E-cadherin was essential for the oncogenic effects of LOC284454 on the invasion and migration of HCC cells. It is possible that E-cadherin is not the only downstream regulator of LOC284454. Further investigations of the downstream regulation mechanisms of LOC284454 are required in the future. However, to the best of our knowledge, the present study was the first to reveal a direct interaction between EZH2 and LOC284454 in HCC by RIP, suggesting that LOC284454 may modulate the enrichment of EZH2 in the E-cadherin mRNA promoter region, which may markedly inhibit E-cadherin expression. Thus, the findings of the present study may contribute to the understanding of the pathogenesis of HCC.

In summary, the present study identified the role of LOC284454 in HCC and proposed that the LOC284454/EZH2/E-cadherin signaling pathway may be a novel therapeutic target for patients with HCC.

Acknowledgements

Not applicable.

Funding

The present study was funded by the National Natural Science Foundation of China (grant no. 82003122) and the Natural Science Foundation of Shaanxi Province (grant no. 2019JQ-128).

Availability of data and materials

The datasets used and/or analyzed during the present study are available from the corresponding author on reasonable request.

Authors' contributions

LH collected the clinical samples, performed most of the experiments and designed the study. WZ performed the experiments and the statistical analysis. FW assisted with the design of the study and drafting of the manuscript. The authenticity of the raw data has been assessed by WZ and FW. All authors have read and approved the final version of the manuscript.

Ethics approval and consent to participate

The present study was approved by the Ethics Committee of Xi'an Jiaotong University (Xi'an, China), and written informed consent was provided by participants before the examination phase. The study complied with the principles of the Declaration of Helsinki.

Patient consent for publication

Not applicable.

Competing interests

The authors declare that they have no competing interests.

References

1. Chaudhari VA, Khobragade K, Bhandare M and Shrikhande SV: Management of fibrolamellar hepatocellular carcinoma. Chin Clin Oncol 7: 51, 2018.
2. Thompson AI, Conroy KP and Henderson NC: Hepatic stellate cells: Central modulators of hepatic carcinogenesis. BMC Gastroenterol 15: 63, 2015.
3. Petruzziello A: Epidemiology of hepatitis B virus (HBV) and hepatitis C virus (HCV) related hepatocellular carcinoma. Open Virol J 12: 26-32, 2018.
4. Ponting CP, Oliver PL and Reik W: Evolution and functions of long noncoding RNAs. Cell 136: 629-641, 2009.
5. Jiang X and Liu W: Long noncoding RNA highly upregulated in liver cancer activates p53-p21 pathway and promotes nasopharyngeal carcinoma cell growth. DNA Cell Biol 36: 596-602, 2017.
6. Liao K, Qian Z, Zhang S, Chen B, Li Z, Huang R, Cheng L, Wang T, Yang R, Lan J, *et al*: The LGMN pseudogene promotes tumor progression by acting as a miR-495-3p sponge in glioblastoma. Cancer Lett 490: 111-123, 2020.
7. García-Venzor A, Mandujano-Tinoco EA, Ruiz-Silvestre A, Sánchez JM, Lizarraga F, Zampedri C, Melendez-Zajgla J and Maldonado V: lncMat2B regulated by severe hypoxia induces cisplatin resistance by increasing DNA damage repair and tumor-initiating population in breast cancer cells. Carcinogenesis 41: 1485-1497, 2020.
8. Zhang Y, Huang W, Yuan Y, Li J, Wu J, Yu J, He Y, Wei Z and Zhang C: Long non-coding RNA H19 promotes colorectal cancer metastasis via binding to hnRNPA2B1. J Exp Clin Cancer Res 39: 141, 2020.
9. Das M, Renganathan A, Dighe SN, Bhaduri U, Shettar A, Mukherjee G, Kondaiah P and Satyanarayana Rao MR: DDX5/p68 associated lncRNA LOC284454 is differentially expressed in human cancers and modulates gene expression. RNA Biol 15: 214-230, 2018.
10. Fan C, Wang J, Tang Y, Zhang S, Xiong F, Guo C, Zhou Y, Li Z, Li X, Li Y, *et al*: Upregulation of long non-coding RNA LOC284454 may serve as a new serum diagnostic biomarker for head and neck cancers. BMC Cancer 20: 917, 2020.
11. Fan C, Tang Y, Wang J, Wang Y, Xiong F, Zhang S, Li X, Xiang B, Wu X, Guo C, *et al*: Long non-coding RNA LOC284454 promotes migration and invasion of nasopharyngeal carcinoma via modulating the Rho/Rac signaling pathway. Carcinogenesis 40: 380-391, 2019.
12. Nieto MA, Huang RY, Jackson RA and Thiery JP: EMT: 2016. Cell 166: 21-45, 2016.

13. Creighton CJ, Gibbons DL and Kurie JM: The role of epithelial-mesenchymal transition programming in invasion and metastasis: A clinical perspective. Cancer Manag Res 5: 187-195, 2013.
14. Han LL, Jia L, Wu F and Huang C: Sirtuin6 (SIRT6) promotes the EMT of hepatocellular carcinoma by stimulating autophagic degradation of E-cadherin. Mol Cancer Res 17: 2267-2280, 2019.
15. Zhou W, Gong L, Wu Q, Xing C, Wei B, Chen T, Zhou Y, Yin S, Jiang B, Xie H, *et al*: PHF8 upregulation contributes to autophagic degradation of E-cadherin, epithelial-mesenchymal transition and metastasis in hepatocellular carcinoma. J Exp Clin Cancer Res 37: 215, 2018.
16. Lee CH, Yu JR, Granat J, Saldaña-Meyer R, Andrade J, LeRoy G, Jin Y, Lund P, Stafford JM, Garcia BA, *et al*: Automethylation of PRC2 promotes H3K27 methylation and is impaired in H3K27M pediatric glioma. Genes Dev 33: 1428-1440, 2019.
17. Ding J, Li J, Wang H, Tian Y, Xie M, He X, Ji H, Ma Z, Hui B, Wang K and Ji G: Long noncoding RNA CRNDE promotes colorectal cancer cell proliferation via epigenetically silencing DUSP5/CDKN1A expression. Cell Death Dis 8: e2997, 2017.
18. Lian Y, Yan C, Xu H, Yang J, Yu Y, Zhou J, Shi Y, Ren J, Ji G and Wang K: A novel lncRNA, LINC00460, affects cell proliferation and apoptosis by regulating KLF2 and CUL4A expression in colorectal cancer. Mol Ther Nucleic Acids 12: 684-697, 2018.
19. Kumar MB, Lu JJ, Loh KS, Chong LM, Soo R, Goh BC, Tan KS and Shakespeare TP: Tailoring distant metastatic imaging for patients with clinically localized undifferentiated nasopharyngeal carcinoma. Int J Radiat Oncol Biol Phys 58: 688-693, 2004.
20. Cantù G, Bimbi G, Miceli R, Mariani L, Colombo S, Riccio S, Squadrelli M, Battisti A, Pompilio M and Rossi M: Lymph node metastases in malignant tumors of the paranasal sinuses: Prognostic value and treatment. Arch Otolaryngol Head Neck Surg 134: 170-177, 2008.
21. Livak KJ and Schmittgen TD: Analysis of relative gene expression data using real-time quantitative PCR and the 2(-Delta Delta C(T)) method. Methods 25: 402-408, 2001.
22. Zhang Q, Wang WW, Xu TH and Xu ZF: Highly expressed long non-coding RNA DUXAP10 promotes proliferation of ovarian cancer. Eur Rev Med Pharmacol Sci 22: 314-321, 2018.
23. Oka H, Shiozaki H, Kobayashi K, Inoue M, Tahara H, Kobayashi T, Takatsuka Y, Matsuyoshi N, Hirano S, Takeichi M, *et al*: Expression of E-cadherin cell adhesion molecules in human breast cancer tissues and its relationship to metastasis. Cancer Res 53: 1696-1701, 1993.
24. Schipper JH, Frixen UH, Behrens J, Unger A, Jahnke K and Birchmeier W: E-cadherin expression in squamous cell carcinomas of head and neck: Inverse correlation with tumor dedifferentiation and lymph node metastasis. Cancer Res 51: 6328-6337, 1991.
25. Li X, Zhang F, Ma J, Ruan X, Liu X, Zheng J, Liu Y, Cao S, Shen S, Shao L, *et al*: NCBP3/SNHG6 inhibits GBX2 transcription in a histone modification manner to facilitate the malignant biological behaviour of glioma cells. RNA Biol 26: 1-17, 2020.
26. Zhang F, Ruan X, Ma J, Liu X, Zheng J, Liu Y, Liu L, Shen S, Shao L, Wang D, *et al*: DGCR8/ZFAT-AS1 promotes CDX2 transcription in a PRC2 complex-dependent manner to facilitate the malignant biological behavior of glioma cells. Mol Ther 28: 613-630, 2020.
27. Wang X, Goodrich KJ, Conlon EG, Gao J, Erbse AH, Manley JL and Cech TR: C9orf72 and triplet repeat disorder RNAs: G-quadruplex formation, binding to PRC2 and implications for disease mechanisms. RNA 25: 935-947, 2019.
28. He W, Yu Y, Huang W, Feng G and Li J: The pseudogene DUXAP8 promotes colorectal cancer cell proliferation, invasion, and migration by inducing epithelial-mesenchymal transition through interacting with EZH2 and H3K27me3. Onco Targets Ther 13: 11059-11070, 2020.
29. Chen WW, Qi JW, Hang Y, Wu JX, Zhou XX, Chen JZ, Wang J and Wang HH: Simvastatin is beneficial to lung cancer progression by inducing METTL3-induced m6A modification on EZH2 mRNA. Eur Rev Med Pharmacol Sci 24: 4263-4270, 2020.
30. Chen Y, Yang F, Fang E, Xiao W, Mei H, Li H, Li D, Song H, Wang J, Hong M, *et al*: Circular RNA circAGO2 drives cancer progression through facilitating HuR-repressed functions of AGO2-miRNA complexes. Cell Death Differ 26: 1346-1364, 2019.
31. Gu X, Li H, Sha L and Zhao W: A prognostic model composed of four long noncoding RNAs predicts the overall survival of Asian patients with hepatocellular carcinoma. Cancer Med 9: 5719-5730, 2020.
32. Wang H, Huo X, Yang XR, He J, Cheng L, Wang N, Deng X, Jin H, Wang N, Wang C, *et al*: STAT3-mediated upregulation of lncRNA HOXD-AS1 as a ceRNA facilitates liver cancer metastasis by regulating SOX4. Mol Cancer 16: 136, 2017.
33. Liu J, Xu R, Mai SJ, Ma YS, Zhang MY, Cao PS, Weng NQ, Wang RQ, Cao D, Wei W, *et al*: lncRNA CSMD1-1 promotes the progression of Hepatocellular Carcinoma by activating MYC signaling. Theranostics 10: 7527-7544, 2020.
34. Wang J, Choi JM, Holehouse AS, Lee HO, Zhang X, Jahnel M, Maharana S, Lemaitre R, Pozniakovsky A, Drechsel D, *et al*: A molecular grammar governing the driving forces for phase separation of Prion-like RNA binding proteins. Cell 174: 688-699.e16, 2018.
35. Dominguez D, Freese P, Alexis MS, Su A, Hochman M, Palden T, Bazile C, Lambert NJ, Van Nostrand EL, Pratt GA, *et al*: Sequence, structure, and context preferences of human RNA binding proteins. Mol Cell 70: 854-867.e9, 2018.
36. Holmqvist E, and Vogel J: RNA-binding proteins in bacteria. Nat Rev Microbiol 16: 601-615, 2018.
37. Zhu Z, Xu L, Wan Y, Zhou J, Fu D, Chao H, Bao K and Zeng T: Inhibition of E-cadherin expression by lnc-RNA H19 to facilitate bladder cancer metastasis. Cancer Biomark 22: 275-281, 2018.
38. Chen Z, Wu J, Huang W, Peng J, Ye J, Yang L, Yuan Y, Chen C, Zhang C, Cai S, *et al*: Long non-coding RNA RP11-789C1.1 suppresses epithelial to mesenchymal transition in gastric cancer through the RP11-789C1.1/miR-5003/E-cadherin axis. Cell Physiol Biochem 47: 2432-2444, 2018.
39. He R, Zhang FH and Shen N: lncRNA FEZF1-AS1 enhances epithelial-mesenchymal transition (EMT) through suppressing E-cadherin and regulating WNT pathway in non-small cell lung cancer (NSCLC). Biomed Pharmacother 95: 331-338, 2017.
40. Liu L, Xu Z, Zhong L, Wang H, Jiang S, Long Q, Xu J and Guo J: Enhancer of zeste homolog 2 (EZH2) promotes tumour cell migration and invasion via epigenetic repression of E-cadherin in renal cell carcinoma. BJU Int 117: 351-362, 2016.
41. Tong ZT, Cai MY, Wang XG, Kong LL, Mai SJ, Liu YH, Zhang HB, Liao YJ, Zheng F, Zhu W, *et al*: EZH2 supports nasopharyngeal carcinoma cell aggressiveness by forming a co-repressor complex with HDAC1/HDAC2 and Snail to inhibit E-cadherin. Oncogene 31: 583-594, 2012.
42. Niu G, Zhuang H, Li B and Cao G: Long noncoding RNA linc-UBC1 promotes tumor invasion and metastasis by regulating EZH2 and repressing E-cadherin in esophageal squamous cell carcinoma. J BUON 23: 157-162, 2018.
43. Petrova YI, Schecterson L and Gumbiner BM: Roles for E-cadherin cell surface regulation in cancer. Mol Biol Cell 27: 3233-3244, 2016.
44. Wong SHM, Fang CM, Chuah LH, Leong CO and Ngai SC: E-cadherin: Its dysregulation in carcinogenesis and clinical implications. Crit Rev Oncol Hematol 121: 11-22, 2018.
45. Onder TT, Gupta PB, Mani SA, Yang J, Lander ES and Weinberg RA: Loss of E-cadherin promotes metastasis via multiple downstream transcriptional pathways. Cancer Res 68: 3645-3654, 2008.
46. Zhai B, Yan HX, Liu SQ, Chen L, Wu MC and Wang HY: Reduced expression of E-cadherin/catenin complex in hepatocellular carcinomas. World J Gastroenterol 14: 5665-5673, 2008.
47. Qiu Y, Liu Y, Li WH, Zhang HQ, Tian XX and Fang WG: P2Y2 receptor promotes the migration and invasion of breast cancer cells via EMT-related genes Snail and E-cadherin. Oncol Rep 39: 138-150, 2018.
48. Theys J, Jutten B, Habets R, Paesmans K, Groot AJ, Lambin P, Wouters BG, Lammering G and Vooijs M: E-Cadherin loss associated with EMT promotes radioresistance in human tumor cells. Radiother Oncol 99: 392-397, 2011.
49. Menezes SV, Fouani L, Huang MLH, Geleta B, Maleki S, Richardson A, Richardson DR and Kovacevic Z: The metastasis suppressor, NDRG1, attenuates oncogenic TGF-β and NF-κB signaling to enhance membrane E-cadherin expression in pancreatic cancer cells. Carcinogenesis 40: 805-818, 2019.